Mortality estimate driven by population abundance field data in a stage-structured demographic model. The case of *Lobesia botrana*

S. Pasquali*, C. Soresina†, E. Marchesini‡

November 17, 2021

Abstract

Simulating the population dynamics of a stage-structured population requires the knowledge of development, mortality and fecundity rate functions characterizing the species. In general, development and fecundity can satisfactorily be estimated starting from literature data. Unfortunately, this is often not the case for the mortality function due to the lack of experimental data. To overcome this problem, we estimate the mortality rate function from field data on the abundance of the species. The mortality is expressed as a linear combination of cubic splines and the estimation method allows to determine its coefficients taking into account the observations measurement error. Moreover, the variability in the estimate is quantified using the confidence bands for both mortality and dynamics. The presented method allows obtaining a more flexible shape for the mortality rate functions compared with previous methods applied to the same pest. The method has been applied to the case of *Lobesia botrana*, the main pest in the European vineyards, with abundance data collected for five consecutive years in an experimental field in the North of Italy. Data collected over three years are used to estimate the mortality and to analyse the variability in the estimate and its effects on the population dynamics, while the other two datasets are used to validate the model simulating the dynamics using the estimated mortality.

Keywords: Stage-structured population, Physiollogically-based demographic model, Mortality estimate, Population abundance time-series, *Lobesia botrana*

1 Introduction

Population dynamics models play an important role in pest control. Predictive information of the temporal dynamics of a pest population can help decision-makers in the choice of the best strategy in terms of the application of phytosanitary treatments. This is a fundamental task in light of the Directive 2009/128/EC on the sustainable use of pesticides in Europe.

To realistically describe the population dynamics of a pest, it is necessary to take into account climatic factors, phenology of the plant and, in general, physical-biological characteristics of the environment in the site of interest. All these factors affect the biology of the species, mathematically described by biodemographic functions, namely development, mortality and reproduction rate functions. The dynamics of the species can be represented by mechanistic models that allow describing the physiological response of the species to environmental driving variables. These models are known

*CNR-IMATI "Enrico Magenes", via Alfonso Corti 12, 20133 Milano, Italy - sara.pasquali@mi.imati.cnr.it

†Institut für Mathematik und Wissenschaftliches Rechnen, Universität Graz, Heinrichstr. 36, 8010 Graz, Austria - cinzia.soresina@uni-graz.at - ORCiD: 0000-0002-0247-3632

‡AGREA S.r.l. Centro Studi, via Garibaldi 5/16, 37057 S. Giovanni Lupatoto (VR), Italy - enrico.marchesini@agrea.it

as physiologically-based models (Gutierrez, 1996) and describe the species life history through the biodemographic functions. Each individual of the population is characterized by a physiological age which is a biometric descriptor of its development. Physiologically-based models allow representing a non-linear relationship between environmental drivers and physiological processes describing the population dynamics, capture processes at different trophic levels, and supply predictions on pest population dynamics taking into account biological and ecological variability. Especially when combined with weather forecasts, they can be used to predict the population dynamics, phenology and distribution of a pest. Model outputs can guide farmers in the rational use of pesticides. For these reasons and, in particular, for the ability to provide information on the dynamics and the phenology of a species, they are important tools to support Integrated Pest Management (Gutierrez et al., 2012; Gutierrez & Wilson, 1989; Sporleder et al., 2009).

Physiologically-based models can be used to predict both the cumulated emergence of individuals in the different stages (phenological models) and the population abundance over time (demographic models). Phenological models can be applied starting from a fixed initial condition considering development rate functions only, but also mortality and fecundity rate functions can be introduced. Effects of mortality and fecundity rate functions in phenological models are discussed in Pasquali et al. (2019). Physiologically-based demographic models (PBDMs) allow predicting population abundance over time, taking into account the environmental variables influencing the dynamics of a species. These mechanistic models have been used for a long time (see for instance De Wit & Goudriaan (1974); Gutierrez et al. (1975); McDonald et al. (1989); Wang et al. (1977)).

The life-cycle of an insect is characterized by several immature stages and one adult reproductive stage. Each developmental stage responds in different ways with respect to biotic and abiotic driver. Most of the pests are dangerous for the crop only in a particular phase of their lifecycle. Then, it is often useful to consider the population organized in stages, through the so-called stage-structured population models (Cushing, 1998; Iannelli, 1994; Iannelli & Milner, 2010). Each stage is characterized by development and mortality rate functions, while the adult stage is defined also through a reproductive function.

PBDMs have been widely used in the last years to describe pest population dynamics for stage-structured populations (Ainseba et al., 2011; Blum et al., 2018; Ewing et al., 2016; Gilioli et al., 2016, 2017, 2014; Marini et al., 2016; Metz & Diekmann, 1986; Pasquali et al., 2020; Rossini et al., 2020). Here we consider a physiologically-based demographic model for a stage-structured population described by a system of partial differential equations which is a particular case of a more general stage-structured population model presented in Buffoni & Pasquali (2007). The output of the model is the abundance of the population in each stage in time and physiological age, defined as the percentage of development within a stage. It is based on stage-specific biodemographic functions dependent on environmental variables, mainly temperature. A reliable estimate of the biodemographic functions allows obtaining a reliable model for population dynamics.

In general, these rate functions are estimated starting from literature data on the biology of the species (for instance, temperature-dependent duration within a stage for the development function, number of eggs produced by an adult female at different temperatures for the fecundity function). Starting from these data, a simple least square method allows estimating the parameters of a biodemographic function of a given functional form. Unfortunately, data for the estimation of the mortality functions are often lacking in the literature. In this case, different methods of estimation can be applied (see for instance Wood & Nisbet (2013) for a survey of mortality estimation methods). When laboratory data on the mortality rate are not available, the mortality estimate can rely on the knowledge of time series data on population dynamics. Different methods to estimate mortality starting from population dynamics time series data have been proposed in the last years. Ellner et al. (2002) proposed a non-parametric regression model, Picart & Ainseba (2011) solved the problem using a numerical analysis based on a Quasi-Newton method, in Gilioli et al. (2016) a method based on least squares

was presented, while in Lanzarone et al. (2017) a Bayesian estimation method was described. In the last two approaches, a functional form for the mortality is required and the estimate concerns only parameters appearing in these functions. In particular, the authors introduced mortality composed of two terms: an intrinsic temperature-dependent (abiotic) mortality depending on the development rate function, and a constant generation-dependent extrinsic mortality likely related to external natural control factors, to be estimated using time series field data on the population dynamics. Ainseba et al. (2011) also proposed mortality rate functions of a known form depending on both environmental variables and age. Assuming the mortality of a known functional form can be restrictive in some cases, where having more flexibility for the behavior of the mortality rate function with respect to the temperature is preferable. We decided to follow the approach proposed by Wood (2001) which does not require a functional form, but rather expresses the mortality as a linear combination of elements of a suitable basis. The parameter vector containing the coefficient of the linear combination is estimated by minimizing a weighted least squares term that measures the "distance" between the simulated and the observed population abundance. Different weights can be considered for the various stages of the population and/or for the various generations. Here, differently from Wood (2001), we modify the functional to be minimized to take into account the measurement error typical of field observations. The new objective is to minimize the sum of the weighted "distance" between the simulated abundance and the observations range of variability. Furthermore, also the variability in the mortality estimates has been taken into account and leads to variability in the population dynamics, both quantified through confidence bands. Since the estimator of the parameter vector is a random variable, confidence bands are obtained by drawing a certain number of values for the parameter vector from its distribution.

The mortality estimation method is applied to the case study of the grape berry moth *Lobesia botrana* which is considered one of the most dangerous pests in European vineyards. The description of the population dynamics of the grape berry moth has been widely studied in the past (Ainseba et al., 2011; Baumgärtner & Baronio, 1988; Gutierrez et al., 2012; Gilioli et al., 2016). In our study, we consider four developmental stages for *L. botrana* population: eggs, larvae, pupae, and adults. To check the convergence of the estimation method, we initially consider the case of population abundances simulated by the model. More precisely, we fix the mortality rate functions of the different stages (in particular, we consider "artificial" mortalities with a bathtub shape) and generate the abundances in all the stages from the population dynamics model obtained with these mortalities and the known development and fecundity rate functions. When we apply the estimation method, starting from the simulated abundances, we correctly reconstruct the mortality rate functions, which means that the estimation procedure is suitable for obtaining a reliable approximation of the mortality rate functions. Then the method is applied to a field case. Data on population abundances for all the stages of the grape berry moth have been collected in Colognola ai Colli (Verona, Italy) in the period 2008–2012 for the cultivar Garganega. The dataset is split into two groups: population abundances of years 2008, 2009 and 2011 are used to estimate the mortality, while data of 2010, and 2012 are used to validate the model. The proposed method allows knowing the behavior of the mortality rates as a function of the temperature. Since the grape berry moth is dangerous only in its larval stage, it is useful to assign a higher weight to this stage when considering the least square term in the estimation procedure. In this way, we aim to obtain better estimates for the abundances of the larvae than for the other stages. This can be useful to the end of grape berry moth control in vineyards (Picart et al., 2011; Picart & Milner, 2014; Picart et al., 2015) because a finer approximation of the number of larvae in the field allows better defining the timing of application of control treatments against the stage. The population dynamics model with the estimated mortalities can be used to forecast the pest abundance. Furthermore, the estimated mortality rate functions, as the other biodemographic functions, represent the physiological responses of the species and thus they are independent from the context of application. Moreover, since the estimation method here described is sufficiently general, it can also be applied to other stage-structured populations.

The paper is organized as follows. In Section 2 the mathematical model describing the dynamics of the population is presented, while in Section 3 the biodemographic functions of the grape berry moth are specified. Section 4 describes the mortality estimation method and the method to determine the confidence bands. In Section 5, the estimation method is applied to the grape berry moth for both the case of simulated data and field data. Finally, Section 6 is devoted to discussion and concluding remarks. The Matlab code implementing the mortality estimation method can be found on GitHub (Pasquali & Soresina, 2021).

2 The mathematical model

The demographic model is based on a system of partial differential equations that allows to obtain the temporal dynamics of the stage-structured population and their distribution over physiological age within each stage. Let

$$\phi^i(t,x)dx = \text{number of individuals in stage } i \text{ at time } t \text{ with physiological age in } (x, x+dx),$$

for $i = 1, 2, ..., s$, where s is the number of stages. Stages from 1 to $s-1$ are immature stages, and stage s represents the reproductive stage (adult individuals). Note that t denotes the chronological time while x represents the physiological age indicating the percentage of development within the stage over time (Buffoni & Pasquali, 2007, 2010, 2013; Di Cola et al., 1999).

Instead of a deterministic setting in which the population dynamics is described through von Foerster equations (Buffoni & Pasquali, 2007), we prefer to consider a stochastic approach that allows taking into account the variability of the development rate among the individuals (Buffoni & Pasquali, 2010, 2013). The dynamics is described in terms of the forward Kolmogorov equations (Gardiner, 1986; Carpi & Di Cola, 1988)

$$\frac{\partial \phi^i}{\partial t} + \frac{\partial}{\partial x}\left[v^i(t)\phi^i - \sigma^i \frac{\partial \phi^i}{\partial x}\right] + m^i(t)\phi^i = 0, \quad t > t_0,\ x \in (0,1), \tag{1}$$

$$\left[v^i(t)\phi^i(t,x) - \sigma^i \frac{\partial \phi^i}{\partial x}\right]_{x=0} = F^i(t), \tag{2}$$

$$\left[-\sigma^i \frac{\partial \phi^i}{\partial x}\right]_{x=1} = 0, \tag{3}$$

$$\phi^i(t_0,x) = \hat{\phi}^i(x), \tag{4}$$

where $i = 1, 2, ...s$, $v^i(t)$ and $m^i(t)$ are the stage-specific development and mortality rates, respectively, assumed to be independent of the age x; $\hat{\phi}^i(x)$ are the initial conditions (namely the initial distributions of the individuals with respect to the physiological age), while σ^i are constant diffusion coefficients. The boundary condition at $x = 0$ assigns the input flux into stage i, while the boundary condition at $x = 1$ means that the output flux from stage i is due only to the advective component $v^i(t)\phi^i(t,1)$ (Buffoni & Pasquali, 2007). Moreover, the fluxes $F^i(t)$ in the boundary conditions (2) are evaluated as follows. The term $F^1(t)$ is the eggs production flux and is given by

$$F^1(t) = v^s(t) \int_0^1 \beta(t,x)\ \phi^s(t,x)\ dx, \tag{5}$$

where $v^s(t)\beta(t,x)$ is the fertility rate. In particular, we consider

$$v^s(t)\beta(t,x) = b(t)f(x) \;\; eggs/adult\ females\ with\ age\ in\ (x, x+dx)/time\ unit, \tag{6}$$

where $b(t)$ takes into account the effect due to both diet and temperature, and $f(x)$ is the oviposition profile.

The other terms $F^i(t)$, when $i > 1$, are the individual fluxes from stage $i-1$ to stage i and are given by

$$F^i(t) = v^{i-1}(t)\phi^{i-1}(t,1), \quad i > 1. \tag{7}$$

The functions $\phi^i(t,x)$ allow to obtain the number of individuals in stage i at time t:

$$N^i(t) = \int_0^1 \phi^i(t,x)dx.$$

System (1)–(4) requires an explicit formulation (depending on a certain number of parameters) of basic biodemographic rate functions (development, fecundity and mortality) that models the physiological response of individuals to environmental forcing variables. For the grape berry moth, as for all the ectotherms, the temperature is one of the main driving variables influencing individuals physiological responses; then, these biodemographic rate functions are formulated in terms of temperature, which depends on the chronological time. It is also possible to take into account the dependence on other environmental variables (Schmidt et al., 2003).

3 Biodemografic functions for *Lobesia botrana*

Lobesia botrana has a stage-structured population, generally considered composed of four stages: eggs, larvae, pupae and adults ($s = 4$). Each stage is characterized by its own biodemographic functions (development, mortality, and, only for adults, fecundity). We suppose that development and mortality rate functions depend on time only through temperature, while the fecundity rate function depends also on the physiological age, as done in Gilioli et al. (2016). In particular, in this paper we consider the same development rate functions estimated in Gilioli et al. (2016), while for the fecundity rate function we use the function $b(t)$ estimated in Gilioli et al. (2016), but a different expression for the oviposition profile $f(x)$ appearing in (6). Experimental laboratory data are used to estimate developmental and fecundity rates: average duration in a stage at different temperatures for development and the average number of eggs produced by a reproductive female at different temperatures and physiological ages for fecundity. On the contrary mortality rates are very difficult to measure due to continuous reproduction and partially overlapping generations (Manly, 1989; Gilioli et al., 2016). Then, to estimate mortality rate functions we rely on the observed abundances for all four stages of the *L. botrana* population using a modified version of the method proposed by Wood (2001) for formulating and fitting partially specified models.

3.1 Development rate function

The development rate function $v(t)$ appearing in (1) describes the development rate as a function of time through temperature. Typically, there is no development below a low-temperature threshold, while the development rate increases and reaches a maximum at an optimal temperature and then it declines rapidly approaching zero at a thermal maximum (namely the temperature at which life processes can no longer be maintained for prolonged periods of time (Logan et al., 1976)). Several functional expressions have been proposed in the literature to describe development (Kontodimas et al., 2004).

	α^i	β^i	γ^i	δ^i
$i=1$	0.01	0.8051	1.0904	1
$i=2$	0.003	0.662	1.0281	1
$i=3,4$	0.0076	1.7099	1.0929	1.1

Table 1: Parameters of the stage-specific development rate function in (8) for the four stages of *L. botrana*: eggs ($i=1$), larvae ($i=2$), pupae ($i=3$) and adults ($i=4$). We have no data on the duration of the adults, so we assume that the adult development is equal to that of the pupae.~~, the stage biologically most similar to adults.~~

Here, as in Gilioli et al. (2016), we consider a Lactin function (Lactin et al., 1995) to represent the development of all the stages:

$$v^i(t) = \delta^i \max\left\{0, \mathrm{e}^{\alpha^i T(t)} - \mathrm{e}^{\alpha^i T_m - \frac{T_m - T(t)}{\beta^i}} - \gamma^i\right\} \tag{8}$$

where $T_m = 36\,^oC$ is the thermal maximum, α^i is the slope parameter describing the acceleration of the function from the low temperature threshold to the optimal temperature, β^i is the width of the high temperature decline zone, γ^i is a parameter that allows the curve to intersect the abscissa giving a minimum temperature of development, and δ^i is a coefficient of amplification of the curve.

Parameters of the development rate functions are estimated by means of a least square method in Gilioli et al. (2016) using the datasets in Baumgärtner & Baronio (1988); Brière & Pracros (1998), and are reported in Table 1.

3.2 Fecundity rate function

As assumed in (6), eggs production depends both on the physiological age of the adults and on the chronological time through temperature and phenological stage of the host plant as environmental variables. The oviposition profile $f(x)$ in equation (6), as function of the physiological age x, is assumed to be of the functional form

$$f(x) = a x^{r-1} \exp(-cx),$$

where the parameters a, r, c are usually estimated from experimental data, in particular the number of eggs produced by a female at different physiological ages. This class of functions, reproducing the shape of a gamma distribution, is sufficiently general to allow the shift of the peak of fecundity in all values of the physiological age interval, i.e., different sets of parameters a, r, c shift the maximum production of eggs from low physiological ages to high physiological ages.

The term $b(t)$ in equation (6) takes into account the influence of environmental variables, temperature $T(t)$ and phenological stage of the plant $P(t)$, varying with the chronological time. It is expressed by the product (Gilioli et al., 2016; Gutierrez et al., 2012)

$$b(t) = b_0\left(P(t)\right) a_0\left(T(t)\right),$$

where $b_0(\cdot)$ is a step function indicating the insect diet changing over time due to the plant maturation process, and

$$a_0(T) = 1 - \left(\frac{T - T_L - T_0}{T_0}\right)^2$$

captures the effect of temperature. The parameter T_L indicates the minimum temperature of reproduction, while T_0 the half-width of the temperature reproduction interval.

Plant stage	P	$b_0(P)$
Inflorescence	BBCH 53	0.31
Green Berries	BBCH 71	0.48
Maturing fruits	BBCH 81	1
Berries ripe for harvest	BBCH 89	0

Table 2: Values of the step function $b_0(P)$, with steps in four plant phenological stages, following the BBCH-scale (Lorenz et al., 1994).

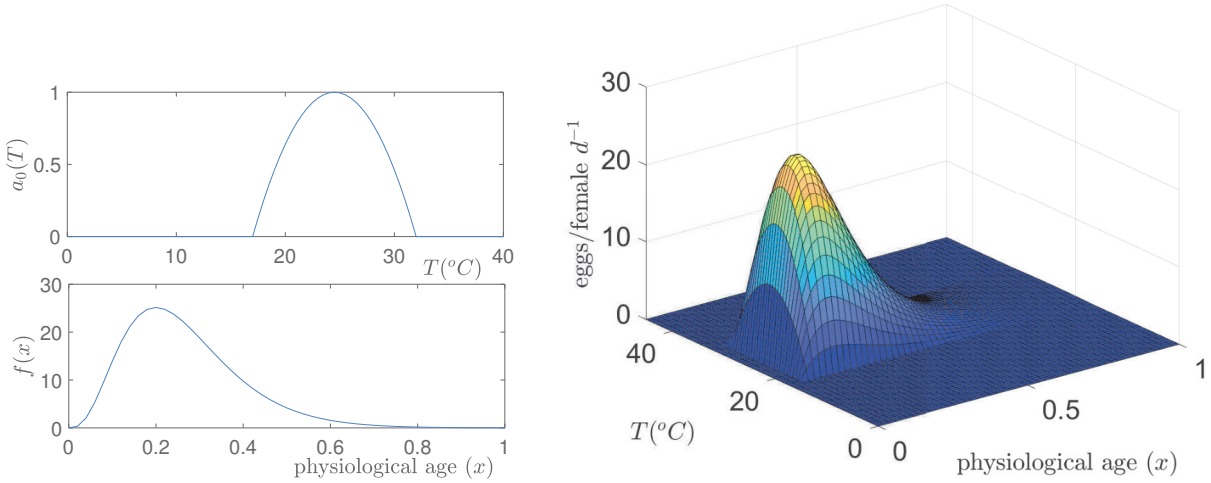

Figure 1: (left panel) Temperature dependent factor and oviposition profile as function of the physiological age. (right panel) Fecundity rate function $(eggs/female\,days^{-1})$ on temperature $(^\circ C)$ and physiological age (dimensionless) for the adult stage of *L. botrana* for $b_0(P) = 1$.

Regarding the case study of *L. botrana*, the parameters appearing in the function $f(x)$ of the fecundity rate are obtained by fitting the corresponding oviposition profile in Baumgärtner & Baronio (1988), suitably converted as a function of the physiological age. In particular, we rescale the fecundity rate function by assuming that physiological age 1 corresponds to 400 degree days in Figure III of Baumgärtner & Baronio (1988). Then, the estimated parameters are

$$a = 74270, \quad r = 4.06, \quad c = 15.33.$$

The values appearing in the function $a_0(T)$, already obtained in Gilioli et al. (2016); Gutierrez et al. (2012) and here reported for the reader's convenience, are

$$T_L = 17\,^oC, \quad T_0 = 7.5\,^oC.$$

The product $f(x)a_0(T)$ $(eggs/female\,day^{-1})$ as a function of temperature $(^\circ C)$ and physiological age x is illustrated in Figure 1. Function $b_0(P(t))$, which depends on the phenological age P of the plant expressed in terms of BBCH-scale (Lorenz et al., 1994), is a step function with steps at the BBCH stages indicated in Table 2 (Gutierrez et al., 2012).

3.3 Mortality rate function

Since mortality rates are very difficult to measure, the functional form of the mortality rate $m(t)$ cannot be easily determined as the development and the fecundity rate functions. In this paper, we consider the mortality $m(t)$ as unknown and we apply a modified version of the estimation method proposed by Wood (2001) for formulating and fitting partially specified models. Thanks to this approach, the obtained mortality carries out both extrinsic and intrinsic mortality factors (see Gilioli et al. (2016)). Moreover, since we want to estimate the mortality rates without assuming a specific functional form for them, we do not specify an analytical expression but only consider some biologically meaningful hypotheses:

- the mortality rate depends on the chronological time through temperature;
- the mortality rate is a non-negative continuous function of temperature;
- the mortality rate is strictly positive at two reference temperatures.

These assumptions will constitute the constraints on the shape of the mortality rates in the sequel.

4 Estimation of the mortality rate function

The estimation method of the mortality rate functions here presented allows dealing with mortality of unknown form, guaranteeing more flexibility for its shape than in Gilioli et al. (2016). To apply this method, we need a dataset of observations of the abundance of the different stages over time. The abundances are collected in the field at different frequencies (for example, weekly) and can concern all the stages or only some stages. These observations are subject to a measurement error depending on the stage because measuring the abundance of a stage might be trickier than for others. For this reason, we want the estimation method from field data to be flexible enough to incorporate such measurement errors.

4.1 The estimation method

We consider system (1)–(4) in which the development functions and the fecundity function are chosen as stated in the previous section, and the mortality rates are unspecified. We want to find the mortality functions $m^i(t)\,(i = 1, \ldots, s)$ that result in the best fit of the model to field data of populations densities for the observed stages. Once the biodemographic functions are fixed, system (1)–(4) can be numerically solved and produce a vector of model estimates $\boldsymbol{\mu}$, representing the population abundances, calculated at the same times of the observations $\boldsymbol{y}$. Usually, observations are affected by errors. In particular, in our case study, it is very difficult to detect insects in some stages of their life, meaning that the observations, namely the field data, could underestimate the real abundances. We denote by $\boldsymbol{u}$ the vector representing the measurement error. Then, we expect the real abundances included in the interval $[\boldsymbol{y}, \boldsymbol{y} + \boldsymbol{u}]$. The goodness of the fit can be quantitatively measured as a weighted sum of squared distance of each observation y_k from the interval $[y_k, y_k + u_k]$:

$$\sum_{k=1}^{d} \max\left\{0, (y_k - \mu_k) w_k (y_k + u_k - \mu_k)\right\},$$

where d is the number of data (obtained as the sum of the number of observations for all the stages) and w_k are the weights associated with each measurement. Then, the best fitting functions m^i are those which minimize this quantity.

The unknown functions m^i can be expressed as linear combination of elements of a suitable basis $\xi_{i,j}(t)$, $i = 1, \ldots, s$, $j = 1, \ldots, n_i$ (for instance, a polynomial or cubic spline basis)

$$m^i(t) = \sum_{j=1}^{n_i} p_{ij}\xi_{ij}(t).$$

Thanks to this choice, the mortality is then very general and it is not limited to a fixed form. The problem of finding the best fitting functions m^i is reduced to finding, under some constraints, the best fitting parameters p_{ij}, $i = 1, \ldots, s$, $j = 1, \ldots, n_i$, collected into the vector $\boldsymbol{p} = [p_{11}, \ldots, p_{1n_1}, \ldots, p_{sn_s}]^T$, which produces the model estimates $\mu(\boldsymbol{p})$. The total number of parameters in vector $\boldsymbol{p}$ is denoted as $n_p = n_1 + \cdots + n_s$. Then our objective is to minimize

$$q(\boldsymbol{p}) = \sum_{k=1}^{d} \max\left\{0, (y_k - \mu_k(\boldsymbol{p}))w_k(y_k + u_k - \mu_k(\boldsymbol{p}))\right\}.$$

The procedure which leads to an estimates of the coefficients $\boldsymbol{p}$ is the following.

1. Given an initial guess of the model parameter vector $\boldsymbol{p}$, denoted by $\boldsymbol{p}^g$, the model equations are numerically solved and model estimates $\boldsymbol{\mu}$ are obtained.

2. By repeatedly solving the model with slight changes in parameters, we obtain an estimate of the $d \times n_p$ matrix $\boldsymbol{J}$ where $J_{ij} = \partial\mu_i\partial p_j$. We use the approximation

$$J_{ij} \sim \frac{\boldsymbol{\mu}_i(\boldsymbol{p}^g + \delta_j\boldsymbol{e}_j) - \boldsymbol{\mu}_i(\boldsymbol{p}^g - \delta_j\boldsymbol{e}_j)}{2\delta_j},$$

   where δ_j is a small number and $\boldsymbol{e}_j$ are vectors of the canonical basis.

3. The quantity $\boldsymbol{\mu}$ and $\boldsymbol{J}$ are used to construct a quadratic model of the fitting objective as a functional of $\boldsymbol{p}$

$$q(\boldsymbol{p}) \sim \sum_{k=1}^{d} \max\left\{0, \left(\hat{y}_k - \sum_{h=1}^{n_p} j_{kh}\boldsymbol{p}_h\right) w_k \left(\hat{y}_k + u_k - \sum_{h=1}^{n_p} j_{kh}\boldsymbol{p}_h\right)\right\}$$

   where $\hat{y}_k = y_k - \mu_k(\boldsymbol{p}^g) + \sum_{h=1}^{n_p} j_{kh}\boldsymbol{p}_h^g$.

4. We find the new direction to modify $\boldsymbol{p}^g$ minimizing, with respect to $\boldsymbol{p}$, the quadratic model of the real fitting objective $q(\boldsymbol{p})$ together with the constraints. A new value of the parameter vector $\boldsymbol{p}^g$ is found.

5. With the new value $\boldsymbol{p}^g$, we iterate steps 1–4 to convergence, obtaining the estimate $\bar{\boldsymbol{p}}$.

It is worthwhile to note that, even though this procedure follows the method proposed in Wood (2001), the quadratic functional to be minimized has been suitably modified to take into account the measurement error in the observations.

4.2 Confidence bands

In addition to the uncertainty on the collected data, the estimation procedure itself produces variability in the mortality rate functions. To account for this effect, we consider confidence bands for both the mortality rate functions and the population dynamics. To this end we observe that, denoting by

$P(t)$	2008	2009	2010	2011	2012
BBCH 53	122	125	126	108	122
BBCH 71	162	150	158	151	162
BBCH 81	218	201	209	192	218
BBCH 89	260	265	274	255	260

Table 3: Days needed from 1^{st} of January to reach the BBCH reported in the first column. The data refers to the vineyard of Garganega located in Colognola ai Colli during the years 2008–2012.

$\hat{\boldsymbol{p}} = \text{argmin}_{\boldsymbol{p}} q(\boldsymbol{p})$ the estimator, the parameter covariance matrix is given by Marsili-Libelli et al. (2003)

$$C_J(\hat{\boldsymbol{p}}) = \frac{q(\hat{\boldsymbol{p}})}{d - n_p} \left(\boldsymbol{J}^T \boldsymbol{W}^{-1} \boldsymbol{J}\right)^{-1}. \tag{9}$$

For large samples, $\hat{\boldsymbol{p}}$ has approximately a multivariate normal distribution with mean $\bar{\boldsymbol{p}}$ and covariance matrix $C_J(\bar{\boldsymbol{p}})$ (Wood, 2001). Since the multivariate normal distribution does not ensure non-negative mortality rate functions, we introduce a more restrictive constraint drawing the parameter from a truncated multivariate normal distribution. We draw a certain number of values of the parameter vector, corresponding to different mortality functions, used to obtain confidence bands for mortality. Then, we run the model for all the mortalities to determine the confidence bands for the population dynamics.

5 The case of *L. botrana*

To estimate the mortality rate functions of the grape berry moth, we need abundance data. We consider two cases. In Subsection 5.1 we generate from model (1)–(4) a dataset of abundances for the four stages of the grape berry moth to check the convergence of the estimation method. Then, we consider the same dataset used in Gilioli et al. (2016) concerning the dynamics of the grape berry moth in a vineyard of Garganega located in Colognola ai Colli (Verona, Veneto Region) in the North-East of Italy, during the time-frame 2008–2012. The experimental field was not treated with pesticides. The abundances have been sampled weekly for eggs, larvae, pupae, and adults. Adult males were detected using pheromone traps, while immature stages were counted on samples of 100 bunches (for a more detailed description of the data collection, see Gilioli et al. (2016)). To estimate the mortality rates functions we used the field data collected at Colognola ai Colli during the three years 2008, 2009 and 2011 (Subsection 5.2); data collected during the other two years (2010 and 2012) were used to validate the model (Subsection 5.3), keeping all the other parameters of development and fecundity fixed. In both cases, development and fecundity rate functions are those defined in Section 3, and the values of the diffusion coefficients are set $\sigma^i = 0.0001,\ i = 1, 2, 3, 4$ as in Gilioli et al. (2016) and Lanzarone et al. (2017) to make the comparison with the other approaches easier. Hourly temperature data, collected by a meteorological station close to the vineyard, are used as a driver environmental variable for the model simulation. The times at which the phenological stage of the plant $P(t)$ reaches the BBCHs reported in Table 2 vary over the years; they are reported in Table 3 for the vineyard of Garganega located in Colognola ai Colli for the years 2008–2012.

It is also important to take into account that observed abundances are subject to a measurement error depending on the stage; for instance, it is very difficult to detect eggs and pupae. In fact, to count first-generation eggs it is necessary to pick up small grape bunches and to analyse them in a laboratory using a stereomicroscope. For the other generations, a magnifying glass is used to observe bunches in

the field and this operation requires particular attention. From the third generation, pupae are under the rhytidome, while second-generation pupae can be hidden either in the grape berries or under the rhytidome, making the detection of this stage particularly difficult. Then, based on the experience of one of the authors in collecting data in vineyards, for eggs and pupae, we consider a measurement error up to 50% of the collected abundance. Larvae are more visible due to the damage they produce, then we suppose to have a measurement error of up to 10% for this stage. These assumptions about measurement error are based on field observations in our specific case. Adults males are caught with pheromone traps, then we assume they are correctly measured. The sex ratio is assumed to be 0.5, as in Gutierrez et al. (2012), therefore the number of males caught in traps is equal to the number of adult females. Moreover, we consider a population composed only of females responsible for reproduction.

The mortality rate functions are expressed as linear combination of cubic B-splines. The basis is built on the nodes $[0, 20, 40]$, being $[0, 40]$ a suitable interval of temperature, and hence it consists in five polynomials $\xi_j(T(t)),\ j = 1, \dots, 5$ defined on this interval. The mortality rates function are

$$m^i(T(t)) = \sum_{j=1}^{5} p_{ij}\xi_j(T(t)), \quad i = 1, \dots, 4.$$

The constraint minimization of $q(\boldsymbol{p})$ (fourth point of the estimation method explained in Section 4.1) has been carried out using the `fmincon` MATLAB routine. In this setting it is possible to include the constraints on the mortality rates (stated in Subsection 3.3) as linear inequalities involving the parameters p_{ij}.

5.1 Method validation

To check the convergence of the estimation method described in the previous subsection, we need a dataset obtained from known biodemographic functions. Then, we generate data of population abundance for three years using the available hourly temperatures in Colognola ai Colli for the years 2008, 2009, 2011. We run the model (1)–(4), using the development and fecundity rate functions defined in Section 3 with an initial condition of 100 adults with physiological age 0 at May 1^{st} and the artificial mortality rate functions represented with red lines in Figure 2, which have a bathtub shape realistic for a mortality rate function. We pick a value of abundance every 10 days, for all the stages, starting from May 1^{st}, up to the end of the year. To reproduce the measurement error, for each abundance we draw a value u from a uniform distribution over the interval $[0, 0.5]$ for eggs and pupae and over the interval $[0, 0.1]$ for the larvae and multiply the abundances by $1 - u$ obtaining the underestimated population abundances. To avoid confusion with the field case, these data are referred to as "artificial observations" and will be used in the estimation procedure to check the convergence of the estimation method proposed. The measurement error also defines the interval of the variability of the artificial observations.

We apply the estimation method considering equal weights for all the data. We have to minimize the sum of the weighted squared differences $q(\boldsymbol{p})$ between simulated dynamics and artificial observations for all three years 2008, 2009, 2011. More precisely, the number of artificial observations will be $d = d_{2008} + d_{2009} + d_{2011}$, where d_Y is the number of artificial observations generated for the year Y (intended as the sum of the observations for all the stages). Applying the method described in Subsection 4.1 we obtain the estimated mortality reported in Figure 2 with a blue continuous line. It can be seen that the estimated mortalities well approximate the artificial mortalities with bathtub shape used to generate data (red dashed lines), in particular in the central part of the temperature interval. For low and high values of temperatures, some differences between the two curves can be observed due to the scarcity of artificial observations for these temperatures which are unlikely in the temperature dataset used here. However, looking at Figure 3, it is evident that these differences do not produce

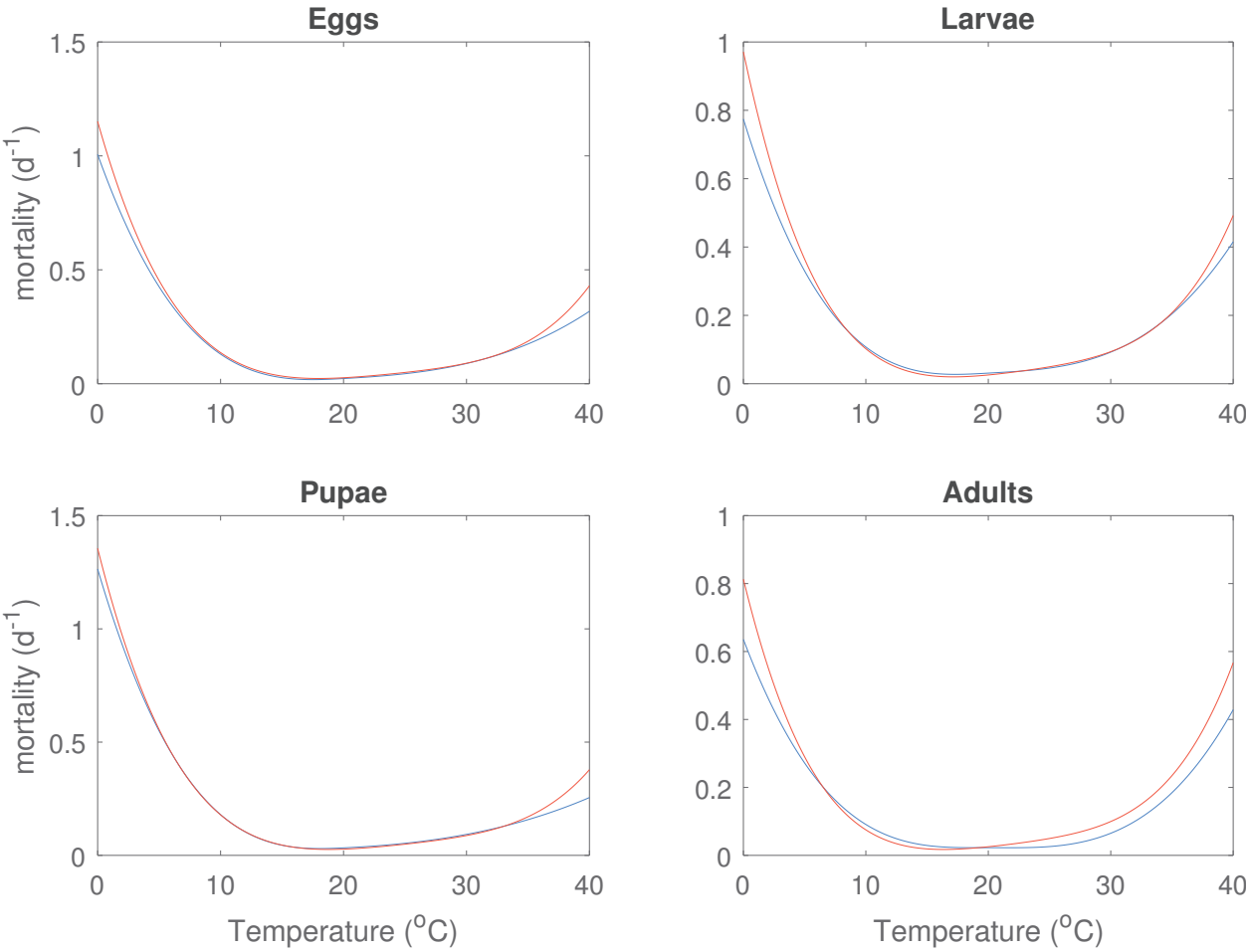

Figure 2: Mortality functions for all the stages of the grape berry moth in case of artificial observations. Red dashed line: artificial mortality rate functions used to generate data; continuous blue line: estimated mortalities. Blue and red lines are very similar, meaning that the estimation algorithm allows obtaining reliable estimates of the mortality rate functions.

significant variations between simulated population dynamics and artificial observations because indeed low and high temperatures are very unlikely in temperate regions (such as Colognola ai Colli) in the period May–September. The simulated dynamics for immature stages, denoted with a continuous blue line in Figure 3, almost perfectly fit the artificial observations, meaning that the simulated trajectories cross nearly all the intervals of variability of the artificial observations, represented by the vertical red intervals in Figure 3. This result shows that the algorithm can provide a reliable approximation of the mortality functions and can be usefully applied to the case of field data. We remark that in this case, we do not report the confidence bands for mortality rate functions and population dynamics because they are extremely thin in both cases.

5.2 Model calibration

In the case of field data, we must collect information on the population densities at the beginning of the season to drive the simulation during the entire growing season. In our study, the number of adults caught by pheromone traps at the first collection date in the favourable season is used as the initial condition of the model. Then, as done in Gilioli et al. (2016), to avoid the extinction of the population

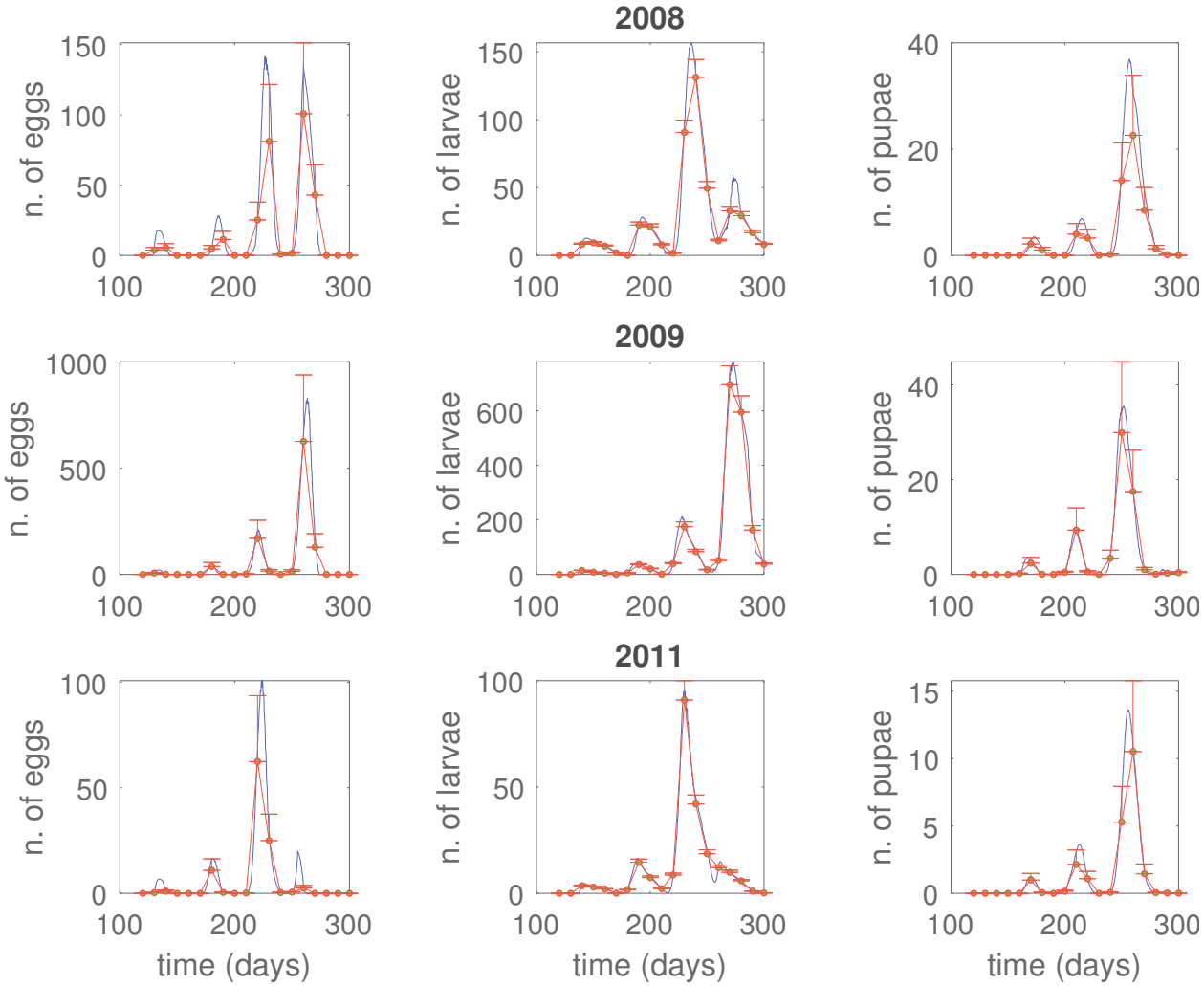

Figure 3: Population dynamics in case of artificial observations. Red points: artificial observations generated from model (1)–(4) using artificial mortalities (red dashed lines in Figure 2) and hourly temperatures recorded in a Garganega vineyard in Colognola ai Colli for the years 2008, 2009, and 2011. Vertical red intervals represent the range of variability of artificial observations (50% of the eggs and pupae abundance, 10% of larval abundance). Blue continuous line: simulated population dynamics obtained with the estimated mortality functions (blue continuous lines in Figure 2).

due to a period of low temperatures, additional inputs are introduced into the system every week on the adults caught by the traps until the first larvae of the first generation are observed.

As in the previous case, we have to minimize the sum of the weighted squared differences $q(\boldsymbol{p})$ between simulated dynamics and observations for all three years 2008, 2009, 2011, with $d = d_{2008} + d_{2009} + d_{2011}$ total observations. As an initial guess for the estimation algorithm, we used a linear combination of cubic B-splines that approximate the mortality rates already used in Gilioli et al. (2016).

In the case of field data we do not consider equal weight for all the stages, but we assign a higher weight to the larval stage. This choice relies on the harmfulness of the larvae that in second-generation cause severe damage to the grapes (Pavan et al., 1998; Pavan & Sbrissa, 1994). Then, it is important to obtain a reliable forecast of the larval abundance, in particular to the end of pest control. Moreover,

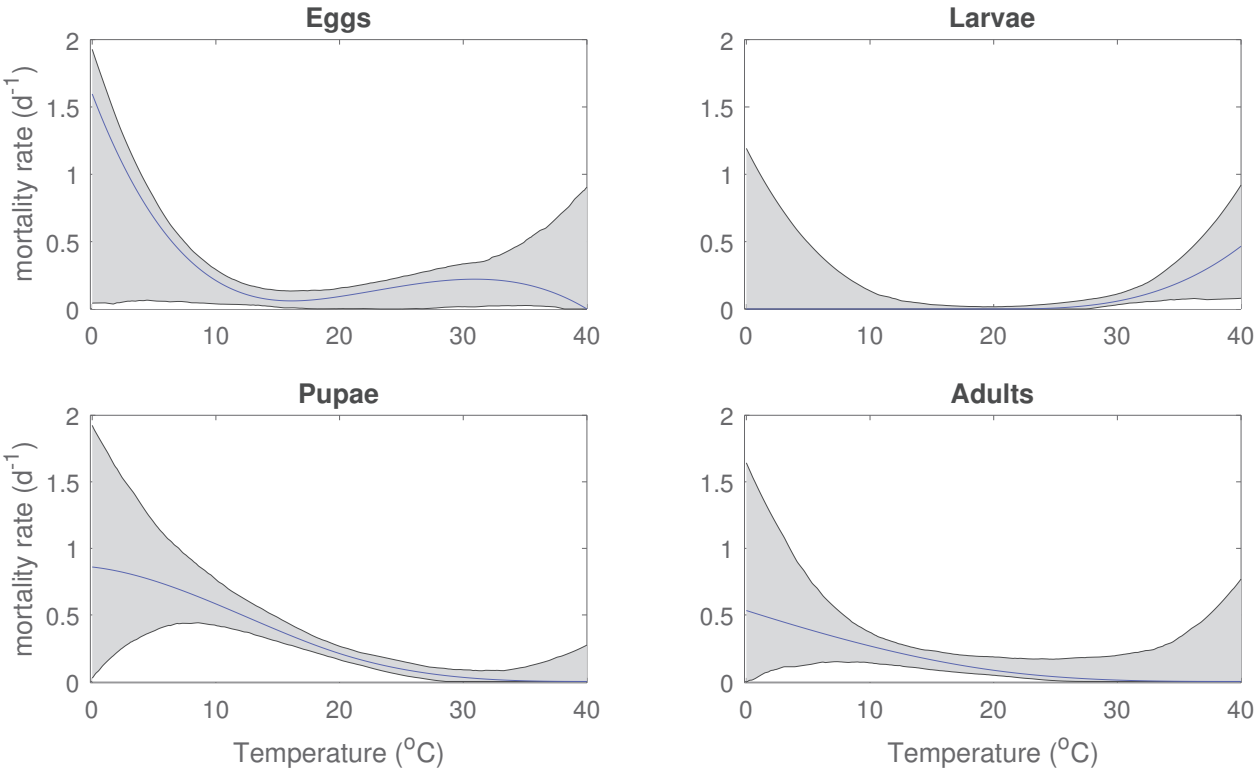

Figure 4: Estimated mortality functions from field data and their 95% confidence bands. Blue continuous lines: estimated mortality functions. Grey area: 95% confidence bands for the mortality rate functions of the different stages of the grape berry moth.

data collected on larvae are more reliable than for the other stages. For all these reasons, the weights assigned to larval observations are one hundred times the weights of the observations assigned to the other stages. To account for the effect of the variability in the parameters estimates, we consider the confidence bands for both the mortality rate functions and the grape berry moth dynamics. In particular, we know that the probability distribution of the parameter $\hat{\boldsymbol{p}}$ can be approximated by a multivariate normal distribution with mean $\bar{\boldsymbol{p}}$ and covariance matrix (9). We draw 500 realisations of the vector parameter from this distribution, that correspond to 500 mortalities for each stage expressed as $\max\{0, \sum_{j=1}^{7} p_{i,j}\xi_{i,j}(t)\}$, because they cannot be negative. The 95% confidence bands of the mortality rate functions are obtained from these 500 mortalities using the MATLAB routine `prctile`. To see the effects of the mortality variability in the population dynamics, we run the model for the 500 mortalities computed to obtain the mortality confidence bands and then we determine the population dynamics bands.

The mortality rate functions obtained in the case of field data and the relative 95% confidence bands are represented in Figure 4. It can be observed that confidence bands are tight in the central part of the temperature interval, that is when temperatures are favourable to the pest growth. This is due to the fact that the temperature datasets here considered contains mainly temperatures between 10 and 35^oC allowing us to obtain a better estimate in this temperature range. Conversely, they are largely outside this range, which corresponds to unlikely temperatures when no data or few data on population abundance are available. Then, there is more uncertainty in estimating mortalities outside the temperature interval $[10^oC, 35^oC]$ and consequently the confidence bands will be larger. Moreover, if a long period of very low temperatures is considered, the population extinct, making uncertain the mortality estimate in this case. The estimated mortalities (blue lines in Figure 4), but especially the

Years	EGGS	LARVAE	PUPAE
2008	0.1999	0.2002	0.1363
2009	0.2835	0.2717	0.2461
2011	0.3741	0.1722	0.4773
Mean	0.2858	0.2147	0.2866

Table 4: NRMSEs for immature stages in the years 2008, 2009 and 2011, relative to Figure 5. The NRMSE measures the distance between the simulated dynamics (continuous blue line) and the observed abundance intervals of variability (red vertical intervals).

upper bounds of the confidence bands (namely the upper bounds of the grey areas) show, for almost all stages, an increase for both increasing and decreasing temperatures. In particular, the upper bounds of the grey areas present a bathtub shape, realistic for a mortality function. This behavior for "extreme" temperatures is in accordance with the mortality proposed in Gilioli et al. (2016) where second-order degree polynomials were used to describe mortality for low and high temperatures. In the central part of the temperature interval (approximately between 10^oC and 35^oC) mortality has lower values in line with the high survival obtained by Brière & Pracros (1998). The estimated larval mortality (blue line) is almost vanishing between 0 and 27^oC, but for cold temperatures it is compensated by high mortalities for the other three stages, which instead have low mortalities for temperatures approaching 40^oC. However, the large variability outside the interval $[10^oC, 35^oC]$ makes the estimated mortalities highly uncertain, allowing for low survival at extreme temperatures, as reported by Brière & Pracros (1998). As in the previous case of artificial observations generated from system (1)–(4), the variability in the mortality for high and low temperatures does not negatively affect the dynamics of the pest because in the period considered here, between mid-April and the end of September, temperatures outside the interval $[10^oC, 35^oC]$ occasionally occur, and therefore the mortality values corresponding to these temperatures occur only a few times. The pest dynamics for the immature stages are reported in Figure 5. We omit the adult stage because adults are sampled differently than immature stages, and moreover, they do not cause direct damage to plants.

The fit of the immature stages is satisfactory, also taking into account the large measurement error we have considered. To quantify the distance between the simulated dynamics and the observed abundance interval of variability, we consider the normalized root mean square error (NRMSE) related to the stage i and year Y, defined as

$$\mathrm{NRMSE}_Y^i = \frac{1}{\max(\boldsymbol{y}_Y^i) - \min(\boldsymbol{y}_Y^i)} \sqrt{\frac{\sum_{k=1}^{d_Y^i} \max\left\{0, (y_k - \mu_k(\bar{\boldsymbol{p}}))\,(y_k + u_k - \mu_k(\bar{\boldsymbol{p}}))\right\}^2}{d_Y^i}}, \tag{10}$$

where $\boldsymbol{y}_Y^i$ denotes the vector of observations in year Y for the stage i, of length d_Y^i. The computed NRMSE for the immature stages in the years 2008, 2009 and 2011 are reported in Table 4. As expected, population dynamics obtained considering a mortality function estimated with a higher weight for larvae present a better fit for the larval stage than for the other stages, as indicated in Table 4 by the mean of the NRMSEs over the years. We also observe that the means of the NRMSE here obtained are lower than those computed for the model in Gilioli et al. (2016) (respectively, 0.9455 for eggs, 0.3062 for larvae, 0.406 for pupae), intended as the distance between the simulated and the observed abundances.

Moreover, taking into account the uncertainty in the estimates, looking at Figure 5 we observe that for all the three considered years the confidence bands for the larval stage include the majority of the observed abundance intervals of variability or cross these intervals. For eggs and pupae, only in

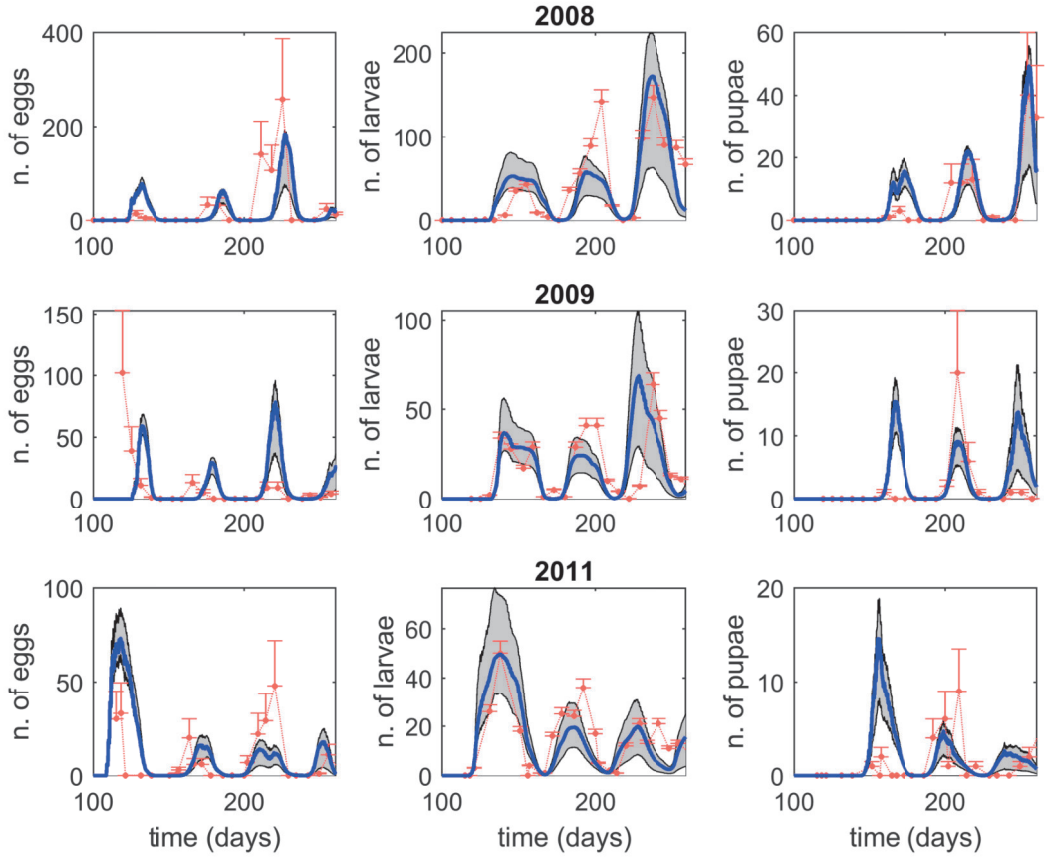

Figure 5: Population dynamics in the case of field data. Red points represent data collected in a Garganega vineyard in Colognola ai Colli for the years 2008, 2009 and 2011, while vertical red intervals indicate the range of variability of observed data (50% of the eggs and pupae abundance, 10% of larval abundance). Note that thin red dotted lines do not correspond to data, but only connects red points. Continuous blue lines inside the grey areas show the dynamics obtained by running system (1)–(4) using the estimated mortalities represented in Figure 4. Grey areas denote the 95% confidence bands for the dynamics of the grape berry moth immature stages.

some cases, the observed values fall in the 95% confidence bands, but the estimated dynamics allow to obtain values for larvae not far from the observed abundance intervals of variability (see values of NRMSEs in Table 4). The confidence bands of the simulated dynamics are particularly large near to the peaks of the dynamics, namely, there is higher uncertainty in the estimates of maximum population abundances, especially for the larval stage, with an impact on pest management strategies.

5.3 Model validation

The datasets recorded in Colognola ai Colli in the years 2010 and 2012 were used to validating the model. We run model (1)–4 using the mortalities estimated in the previous subsection, and keeping all the other parameters of development and fecundity fixed as in the model calibration. The simulated dynamics of the immature stages for the years 2010 and 2012, obtained using the estimated mortality in Figure 4, are represented in Figure 6, while the NRMSEs for all the stages are shown in Table 5. As

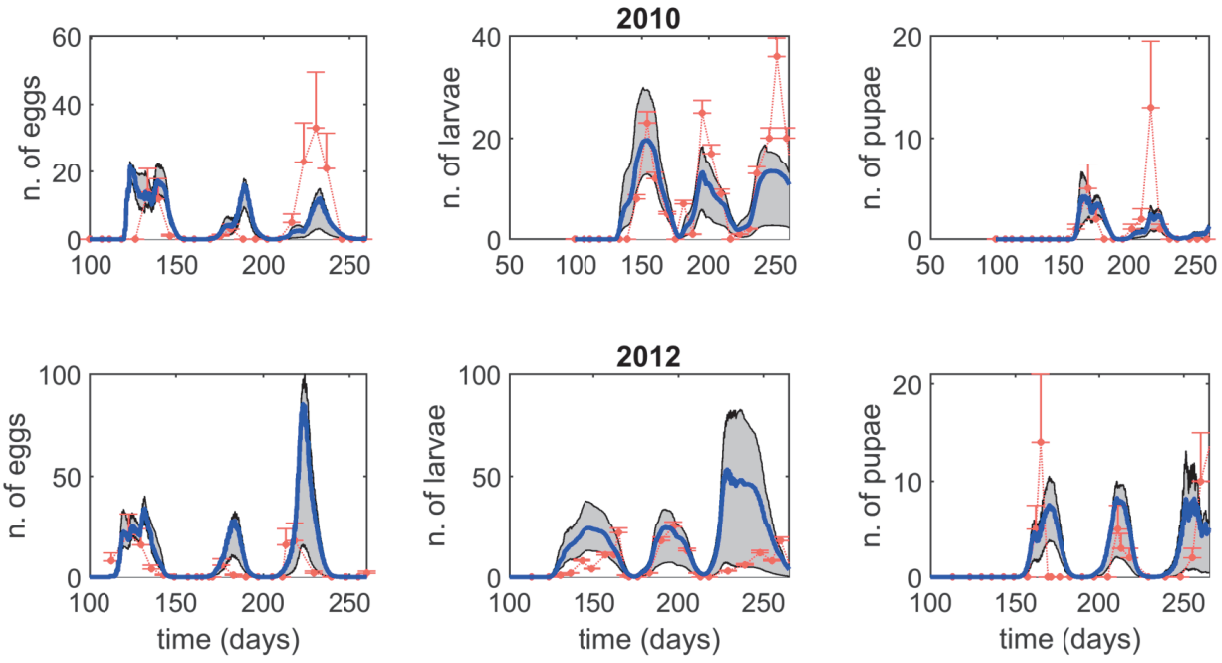

Figure 6: Results of model validation. Red points represent data collected in a Garganega vineyard in Colognola ai Colli for the years 2010, and 2012, while vertical red intervals represent the range of variability of observed data (50% of the eggs and pupae abundance, 10% of larval abundance). Note that thin red dotted lines do not correspond to data, but only connects red points. Continuous blue lines are the dynamics obtained using the estimated mortalities represented in Figure 4. Grey area: 95% confidence bands for the dynamics of the grape berry moth immature stages.

Years	EGGS	LARVAE	PUPAE
2010	0.2527	0.1814	0.1734
2012	0.3186	0.2669	0.2434

Table 5: NRMSEs for immature stages in the years 2010 and 2012, relative to Figure 6. The NRMSE measures the distance between the simulated dynamics (continuous blue line) and the observed abundance intervals of variability (red vertical intervals).

for the calibration phase, we do not consider the adult stage because the data for adults are collected differently than the immature stages and the adults do not cause direct damage to the grapevines.

The NRMSE values in Table 5 are comparable with those in Table 4 relative to the estimation phase, ensuring a satisfactory representation of the immature dynamics (Figure 6). Moreover, as in the previous section, many of the observed values fall into the 95% confidence bands or their variability intervals intersect the confidence bands. These results suggest that the method presented allows obtaining relevant estimates of the stage-specific mortality rate functions. The model implemented using the novel mortality rates provides reliable estimates of the population dynamics of the pest based on temperature. Finally, we remark that the NRMSEs obtained for the years 2010 and 2012 are smaller than the corresponding values computed for the dynamics in Gilioli et al. (2016) for all the immature stages. In fact, the NRMSEs in Gilioli et al. (2016) for the year 2010 are 0.2734 for the eggs, 0.2226

for the larvae and 0.3913 for the pupae, while for the year 2012 are 0.8764 for the eggs, 0.6323 for the larvae and 0.4384 for the pupae.

6 Discussion and concluding remarks

A realistic simulation of the population dynamics relies on the knowledge of the biodemographic functions describing the biology of the species. Development and fecundity rate functions can be estimated using, for example, a simple least square method starting from literature data on duration at different temperatures or data on the average number of eggs produced. However, literature data on mortality are not available because mortality rates are difficult to measure due to continuous reproduction. More complex methods have been developed to estimate biodemographic functions (in particular mortality), based on population dynamics datasets, in case no such data are available (Ellner et al., 2002; Gilioli et al., 2016; Lanzarone et al., 2017; Wood, 2001).

Here we consider the case of the grape berry moth, for which we dispose of 5 years of data on population dynamics in the same location. Three years (2008, 2009 and 2011) are used in the calibration phase to estimate the mortality rate functions. Then, these estimated mortalities are used in the validation phase to test the capacity of the model to predict the observed population dynamics in the years 2010 and 2012. The observations are affected by a measurement error; here we assume that the measurement error is a percentage of the abundance in a stage according to the experience of one of the authors in collecting data in vineyards. To estimate the mortality rate functions of the different stages we propose a method based on the minimization of the sum of weighted squared differences between simulated dynamics and observations. The method relies on the work of Wood (2001), but the functional to be minimized is suitably replaced by a new functional able to take into account the variability in the observations.

The estimation method considered in the present paper has some advantages compared to the method proposed in Gilioli et al. (2016) and Lanzarone et al. (2017) for the grape berry moth mortality estimation. In Gilioli et al. (2016) and Lanzarone et al. (2017) the mortality was represented as the sum of two terms: intrinsic mortality due to abiotic factors and extrinsic mortality due to biotic factors. The intrinsic mortality was estimated using literature data, while for the extrinsic mortality, estimation methods based on population dynamics observations were proposed. Since, as a function of temperature, intrinsic mortality was of a known fixed form, it would not be useful to apply the estimation method proposed here only to extrinsic mortality. In the present paper, mortality is considered as a whole and represented as a linear combination of cubic splines. This assures greater flexibility on the shape of the mortality function. In this work, the splines only depend on temperature which is the main driver, but other environmental variables or biotic factors can be included to further generalize the functions.

To check the convergence of the estimation procedure, an application to a synthetic dataset where data are generated from system (1)–(4) with known mortality rate functions is considered. To mimic the real case, the observations are then "disturbed" by an error. The applied method, using equal weights for all stages, allows us to obtain a precise estimate of both the mortality rate functions and the population dynamics guaranteeing the convergence of the estimation algorithm.

Then, we consider the case of field data. We decided to assign a higher weight to larval observations because, based on the field experience of one of the authors, the measurements of larvae are more precise than for the other immature stages due to the evident damage they produce to vineyards (Pavan et al., 1998; Pavan & Sbrissa, 1994). Then, it is important to have an accurate description of larval dynamics. On the contrary, it is very hard to detect eggs and pupae, then we suppose the abundances in these two stages are subject to 50% errors, while for larvae only a 10% error is considered.

The estimation procedure is subject to variability. In particular, the parameter estimator is a

random variable whose distribution can be approximated by a multivariate normal distribution. Drawing 500 values of the parameter vector from this distribution we can obtain confidence bands for the mortality. Running the model for the 500 mortalities, we obtain the confidence bands also for the population dynamics. The estimated mortalities confidence bands (Figure 4) are thin in the central part of the interval, for favourable temperatures, and large for extreme values of the temperatures showing an increase for high and low-temperature values. This behavior is in agreement with the assumptions made in Gilioli et al. (2016) where the mortality is defined as a second-order degree polynomial for small and large temperatures that infrequently occur.

The simulated population dynamics show a satisfactory approximation of the phenology of the species. A better fit is observed for the larval stage for which a higher weight was considered in the estimation procedure. Indeed, most of the larval observations intervals fall into the 95% confidence bands or their variability ranges intersect the confidence bands. This is important in pest control, mainly based on the control of larvae. Thus, we can obtain a satisfactory larval abundance forecast that allows better planning of pesticides treatments. In our case study, it has been observed that the confidence bands of the simulated dynamics are particularly large near to the peaks of the dynamics. This implies a higher uncertainty in the estimates of maximum population abundances, especially for the larval stage, and it can lead to different strategies in pest management. In detail, it may happen that the simulated larval dynamics (blue lines in Figure 5) does not reach the alert threshold, but the threshold is crossed by the upper limit of the confidence band. We can decide to treat with pesticides when the confidence band cross the alert threshold or when the simulated larval dynamics reaches that threshold, depending on our risk aversion. In the first case, we have a conservative approach and it is more likely to treat with pesticides than in the second case. Once it is decided to follow the simulated dynamics or a limit of the confidence bands, the most appropriate periods to carry out phytosanitary treatments can be easily determined, thus allowing for more rational use of pesticides.

The satisfactory representation of the phenology and dynamics of the species over five years (2008–2012) provides indications about the capacity of the newly estimated mortality rate functions to represent temperature-dependent physiological responses of the species independently from the context of application, as well as development and fecundity rate functions. Thus, it may be possible to use the model to support pest management at other sites. To clarify this issue further, the model should also be tested at other locations. Abundance data from other experimental fields are being collected and will be analysed in future work.

Moreover, the estimation method here presented is sufficiently general to be applied to other pests. The weighted squared differences to be minimized in the estimation procedure allow to differentiate the weights for every single observation. In this way, it is possible to stress the observations relative to a more sensible stage, as in our case, or the observations of one or more, particularly dangerous generations. In addition, it is possible to quantify the range of variability of the dynamics giving a measure of the error of the predicted population dynamics.

In conclusion, the approach adds more realism to the stage-structured population model and it enhances its capability to predict population dynamics, which are key issues in developing strategies for pest management.

Acknowledgements: Support by INdAM-GNFM is gratefully acknowledged by CS. The authors would like to thank Tommaso del Viscio (CNR-IMATI "Enrico Magenes") for technical support.

References

Ainseba, B., Picart, D., & Thiéry, D. (2011). An innovative multistage, physiologically structured, population model to understand the European grapevine moth dynamics. *Journal of Mathematical Analysis and Applications*, *382*(1), 34–46.

Baumgärtner, J. & Baronio, P. (1988). Modello fenologico di volo di *Lobesia botrana* Den. & Schiff. (Lep. Tortricidae) relativo alla situazione ambientale dell'Emilia-Romagna. *Bollettino dell'Istituto di Entomologia della Università di Bologna*, *43*, 157–170.

Blum, M., Nestel, D., Cohen, Y., Goldshtein, E., Helman, D., & Lensky, I. (2018). Predicting Heliothis (*Helicoverpa armigera*) pest population dynamics with an age-structured insect population model driven by satellite data. *Ecological Modelling*, *369*, 1–12.

Brière, J.-F. & Pracros, P. (1998). Comparison of temperature-dependent growth models with the development of *Lobesia botrana* (Lepidoptera: Tortricidae). *Environmental Entomology*, *27*(1), 94–101.

Buffoni, G. & Pasquali, S. (2007). Structured population dynamics: continuous size and discontinuous stage structures. *Journal of Mathematical Biology*, *54*(4), 555–595.

Buffoni, G. & Pasquali, S. (2010). Individual-based models for stage structured populations: formulation of "no regression" development equations. *Journal of Mathematical Biology*, *60*(6), 831–848.

Buffoni, G. & Pasquali, S. (2013). On modeling the growth dynamics of a stage structured population. *International Journal of Biomathematics*, *6*(06), 1350039.

Carpi, M. & Di Cola, G. (1988). Un modello stocastico della dinamica di una popolazione con struttura di età. Quaderno del Dipartimento di Matematica dell'Università di Parma 31, Università di Parma.

Cushing, J. (1998). *An Introduction to Structured Populations Dynamics*. SIAM, Philadelphia.

De Wit, C. & Goudriaan, J. (1974). *Simulation of Ecological Processes*. Centre for Agricultural Publishing and Documentation, Wageningen, the Netherlands.

Di Cola, G., Gilioli, G., & Baumgärtner, J. (1999). Mathematical models for age-structured population dynamics. In C. Huffaker & A. Gutierrez (Eds.), *Ecological Entomology* (pp. 503–534). New York: John Wiley and Sons.

Ellner, S., Seifu, Y., & Smith, R. (2002). Fitting population dynamic models to time-series data by gradient matching. *Ecology*, *83*(8), 2256–2270.

Ewing, D., Cobbold, C., Purse, B., Nunn, M., & White, S. (2016). Modelling the effect of temperature on the seasonal population dynamics of temperate mosquito. *Journal of Theoretical Biology*, *400*, 65–79.

Gardiner, C. (1986). Handbook of stochastic methods for physics, chemistry and the natural sciences. *Applied Optics*, *25*, 3145.

Gilioli, G., Pasquali, S., & Marchesini, E. (2016). A modelling framework for pest population dynamics and management: An application to the grape berry moth. *Ecological Modelling*, *320*, 348–357.

Gilioli, G., Pasquali, S., Martín, P., Carlsson, N., & Mariani, L. (2017). A temperature-dependent physiologically based model for the invasive apple snail *Pomacea canaliculata*. *International Journal of Biometeorology*, *61*, 1899–1911.

Gilioli, G., Pasquali, S., Parisi, S., & Winter, S. (2014). Modelling the potential distribution of *Bemisia tabaci* in Europe in light of the climate change scenario. *Pest Management Science*, *70*, 1611–1623.

Gutierrez, A. (1996). *Applied population ecology: A supply-demand approach*. Wiley, New York.

Gutierrez, A., Falcon, L., Loew, W., Leipzig, P., & Van den Bosch, R. (1975). An analysis of cotton production in California: a model for Acala cotton and the effects of defoliaters on its yields. *Environmental Entomology*, *4*, 125–136.

Gutierrez, A., Ponti, L., Cooper, M., Gilioli, G., Baumgärtner, J., & Duso, C. (2012). Prospective analysis of the invasive potential of the European grapevine moth *Lobesia botrana* (Den. & Schiff.) in California. *Agricultural and Forest Entomology*, *14*(3), 225–238.

Gutierrez, A. & Wilson, L. (1989). Development and use of pest models. In R. Frisbie, K. El-Zik, & L. Wilson (Eds.), *Integrated Pest Management Systems and Cotton Production* (pp. 65–83). New York: Wiley Interscience.

Iannelli, M. (1994). *Mathematical Theory of Age-Structured Population Dynamics*. Giardini, Pisa.

Iannelli, M. & Milner, F. (2010). *The Basic Approach to Age-Structured Population Dynamics: Models, Methods and Numerics*. Springer.

Kontodimas, D., Eliopoulos, P., Stathas, G., & Economou, L. (2004). Comparative temperature-dependent development of *Nephus includens* (kirsch) and *Nephus bisignatus* (boheman)(Coleoptera: Coccinellidae) preying on *Planococcus citri* (risso)(Homoptera: Pseudococcidae): evaluation of a linear and various nonlinear models using specific criteria. *Environmental Entomology*, *33*(1), 1–11.

Lactin, D., Holliday, N., Johnson, D., & Craigen, R. (1995). Improved rate model of temperature-dependent development by arthropods. *Environmental Entomology*, *24*, 68–75.

Lanzarone, E., Pasquali, S., Gilioli, G., & Marchesini, E. (2017). A Bayesian estimation approach for the mortality in a stage-structured demographic model. *Journal of Mathematical Biology*, *75*(3), 1–21.

Logan, J., Wollkind, D., Hoyt, S., & Tanigoshi, L. (1976). An analytic model for description of temperature dependent rate phenomena in arthropods. *Environmental Entomology*, *5*(6), 1133–1140.

Lorenz, D., Eichhorn, K., Bleiholder, H., Klose, R., Meier, U., & Weber, E. (1994). Phänologische Entwicklungsstadien der Weinrebe (*Vitis vinifera* l. ssp. vinifera). Codierung und Beschreibung nach der erweiterten BBCH-Skala. *Wein-Wissenschaft*, *49*(2), 66–70.

Manly, B. (1989). A review of methods for the analysis of stage-frequency data. In L. McDonald, B. Manly, J. Lockwood, & J. Logan (Eds.), *Estimation and Analysis ofInsect Populations* (pp. 3–69). Berlin, Heidelberg, New York: Springer.

Marini, G., Poletti, P., Giacobini, M., Pugliese, A., Merler, S., & Rosà, R. (2016). The role of climatic and density dependent factors in shaping mosquito population dynamics: the case of *Culex pipiens* in Northwestern Italy. *PLOS ONE*, *11*(4), e0154018.

Marsili-Libelli, S., Guerrizio, S., & Checchi, N. (2003). Confidence regions of estimated parameters for ecological systems. *Ecological Modelling*, *165*, 127–146.

McDonald, L., Manly, B., Lockwood, J., & Logan, J. (1989). *Estimation and Analysis of Insect Populations*. Springer.

Metz, J. & Diekmann, O. (1986). *The Dynamics of Physiologically Structured Populations*. Springer–Verlag Berlin Heidelberg.

Pasquali, S., Mariani, L., Calvitti, M., Ponti, L., Chiari, M., Sperandio, G., & Gilioli, G. (2020). Development and calibration of a model for the potential establishment and impact of *Aedes albopictus* in Europe. *Acta Tropica*, *202*(105228).

Pasquali, S. & Soresina, C. (2021). Supplementary material. Matlab scripts implementing the mortality estimation method at `https://github.com/soresina/mortality_estimate`. Accessed September 21, 2021.

Pasquali, S., Soresina, C., & Gilioli, G. (2019). The effects of fecundity, mortality and distribution of the initial condition in phenological models. *Ecological Modelling*, *402*, 45–58.

Pavan, F., Girolami, V., & Sacilotto, G. (1998). Second generation of grape berry moths, *lobesia botrana* (den. & schiff.)(lep., tortricidae) and *eupoecilia ambiguella* (hb.)(lep., cochylidae): Spatial and frequency distributions of larvae, weight loss and economic injury level. *Journal of Applied Entomology*, *122*(1–5), 361–368.

Pavan, R. & Sbrissa, F. (1994). Damage of the grape berry moths, *lobesia botrana* (den. & schiff.) and *eupoecilia ambiguella* (hb.), on late-harvested cultivars in north-eastern italy. *Frustula Entomologica*, 43–53.

Picart, D. & Ainseba, B. (2011). Parameter identification in multistage population dynamics model. *Nonlinear Analysis: Real World Applications*, *12*, 3315–3328.

Picart, D., Ainseba, B., & Milner, F. (2011). Optimal control problem on insect pest populations. *Applied Mathematics Letters*, *24*, 1160–1164.

Picart, D. & Milner, F. (2014). Optimal control in a multistage physiologically structured insect population model. *Applied Mathematics and Computation*, *247*, 573–588.

Picart, D., Milner, F., & Thiéry, D. (2015). Optima treatment schedule in insect pest control in viticulture. *Mathematical Population Studies*, *22*, 172–181.

Rossini, L., Speranza, S., & Contarini, M. (2020). Distributed delay model and von Foerster's equation: different points of view to describe insects' life cycles with chronological age and physiological time. *Ecological Informatics*, 101117.

Schmidt, K., Hoppmann, D., Holst, H., & Berkelmann-Löhnertz, B. (2003). Identifying weather-related covariates controlling grape berry moth dynamics. *EPPO Bulletin*, *33*(3), 517–524.

Sporleder, M., Chavez, D., Gonzales, J., Juarez, H., Simon, R., & Kroschel, J. (2009). ILCYM-insect life cycle modeling: software for developing temperature-based insect phenology models with applications for regional and global pest risk assessments and mapping. In *Proceedings of the 15th Triennial Symposium of the International Society for Tropical Root Crops (ISTRC)*.

Wang, Y., Gutierrez, A., Oster, G., & Daxl, R. (1977). A population model for plantgrowth and development coupling cotton-herbivore interaction. *The Canadian Entomologist*, *109*, 1359–1374.

Wood, S. (2001). Partially specified ecological models. *Ecological Monographs*, *71*(1), 1–25.

Wood, S. & Nisbet, R. (2013). *Estimation of Mortality Rates in Stage-Structured Population*, volume 90. Springer–Verlag Berlin Heidelberg.